Femtosecond filamentation and pulse compression in the wake of molecular alignment

Jian Wu,[1] Hua Cai,[1] Heping Zeng,[1,*] and Arnaud Couairon[2]

[1]*State Key Laboratory of Precision Spectroscopy, East China Normal University, Shanghai 200062, China*
[2]*Centre de Physique Théorique, CNRS, École Polytechnique, F-91128 Palaiseau, France*
**Corresponding author: hpzeng@phy.ecnu.edu.cn*

Received September 8, 2008; accepted September 26, 2008;
posted October 9, 2008 (Doc. ID 101326); published November 7, 2008

We numerically demonstrate that femtosecond filamentation in a molecular gas can be controlled in the wake of molecular alignment following impulsive rotational Raman excitation with a weak pump pulse. The succeeding filamentation dynamics of the collinearly propagating probe pulse is significantly influenced by the spatiotemporally modulated refractive index at the revivals of molecular alignment. The length of the filament generated by the probe pulse can be efficiently increased to obtain an ultrabroad spectrum and a few-cycle pulse via self-compression by tuning its delay to match the molecular alignment revivals. © 2008 Optical Society of America

OCIS codes: 320.7110, 260.5950, 020.2649.

The propagation of intense femtosecond (fs) pulses in transparent nonlinear media (e.g., air) leads to the observation of filaments [1]. Several applications based on filaments were foreseen, such as light detection and ranging techniques [2], laser induced breakdown spectroscopy [3], remote terahertz sources [4], and nonlinear optical processes [5]. It is important to manage an accurate control of the filament features, in particular the filamentation length that was predicted to reach a maximum for a specific pulse duration [6] and could be controlled by adjusting the initial pulse chirp [7]. An additional control parameter exists for all applications based on filamentation in air: in contrast with an atomic gas, air contains diatomic molecules N_2 and O_2, the orientation of which can be manipulated by using impulsive rotational Raman excitation with periodic revivals [8,9]. Field-free molecular alignment has been extensively studied for full-dimensional molecular manipulation [10], molecular orbital reconstruction [11], and high-harmonic generation [12,13].

In this Letter, we numerically demonstrate that filamentation can be controlled by impulsive rotational Raman excitation of nitrogen with a weak femtosecond pump pulse sent in advance of a more intense probe pulse undergoing filamentation. The molecular refractive index seen by the probe pulse is modulated both spatially and temporally depending on the pump-probe delay, which allows for a control of its propagation dynamics. The filament length is shown to be efficiently increased with a significant spectrum broadening and pulse self-compression when the probe delay is properly tuned to match with the molecular alignment revivals.

The propagation for the probe pulse envelope in prealigned molecules is governed by the nonlinear envelope equation in the local reference frame

$$\frac{\partial E}{\partial z} = \frac{i}{2k_0}\left(\frac{\partial^2}{\partial r^2} + \frac{1}{r}\frac{\partial}{\partial r}\right)E - i\frac{k_0^{(2)}}{2}\frac{\partial^2 E}{\partial t^2} + ik_0\delta nE + ik_0 n_2|E|^2E - \frac{\sigma}{2}(1 + i\omega_0\tau_c)\rho E - \frac{\beta_K}{2}|E|^{2K-2}E, \quad (1)$$

where n_0, k_0, and $k_0^{(2)} = \partial^2 k/\partial\omega^2|_{\omega_0}$ are the refractive index, the wave vector, and the coefficient for group velocity dispersion of the probe pulse centered at ω_0, respectively. The cross-section $\sigma \sim e^2/(c\varepsilon_0 m_e \omega_0^2 \tau_c)$ accounts for inverse Bremsstrahlung with collision time τ_c. The quantity $\beta_K = K\hbar\omega_0\rho_0\sigma_K$ is the multiphoton ionization coefficient, K is the number of photons involved in the process, and ρ_0 is the initial molecular density. The electron density ρ is calculated by resolving $\partial\rho/\partial t = \sigma_K|E|^{2K}(\rho_0 - \rho)$ [1]. The orientation dependent refractive index δn and ionization cross-section σ_K are modeled by $\delta n = 0.5(\rho_0\Delta\alpha/n_0) \times (\langle\langle\cos^2\theta\rangle\rangle - 1/3) + \delta n_{\text{rot-Raman}}$ and $\sigma_K = \sigma_{K0}[1 + (1.5a_2 - 3.75a_4)(\langle\langle\cos^2\theta\rangle\rangle - 1/3) + 4.375a_4(\langle\langle\cos^4\theta\rangle\rangle - 1/5)]$ [12], where $\Delta\alpha$ is the polarizability difference [8]. The refractive index δn due to prealigned molecules is evaluated by including the rotational Raman contribution $\delta n_{rot\text{-}Raman}$ and effectively depends on the pump intensity [14,15]. Molecular alignment is characterized by the averaged terms $\langle\langle\cos^2\theta\rangle\rangle$ and $\langle\langle\cos^4\theta\rangle\rangle$ [8], which are equal to 1/3 and 1/5, respectively, for randomly orientated molecules (without pump).

Figures 1(a) and 1(b) show the calculated alignment metrics versus time delay. Here, the pump pulse is assumed to be 50 fs in duration (FWHM) with a peak intensity of 2×10^{13} W/cm^2 at the focus, whose evolution is assumed to obey the basic Gaussian optics. The molecular gas is considered to be pure N_2 with $\rho_0 = 2.5\times10^{19}$ cm^{-3}. As shown in Figs. 1(c) and 1(d), the refractive index and ionization cross section are modulated by closely following the revivals of the molecular alignment. The modulation of the ionization cross section is due to the fact that a parallel oriented diatomic molecule exhibits a double-well potential structure and is therefore easier to be ionized than a perpendicularly oriented one [16,17]. For N_2 exhibiting a positive $\Delta\alpha$, the refractive index of the molecular gas seen by the probe pulse increases (decreases) as the molecules are prealigned parallel (perpendicular) to the field polarization. Figure 1(c) shows that the rotational Raman contribu-

0146-9592/08/222593-3/$15.00

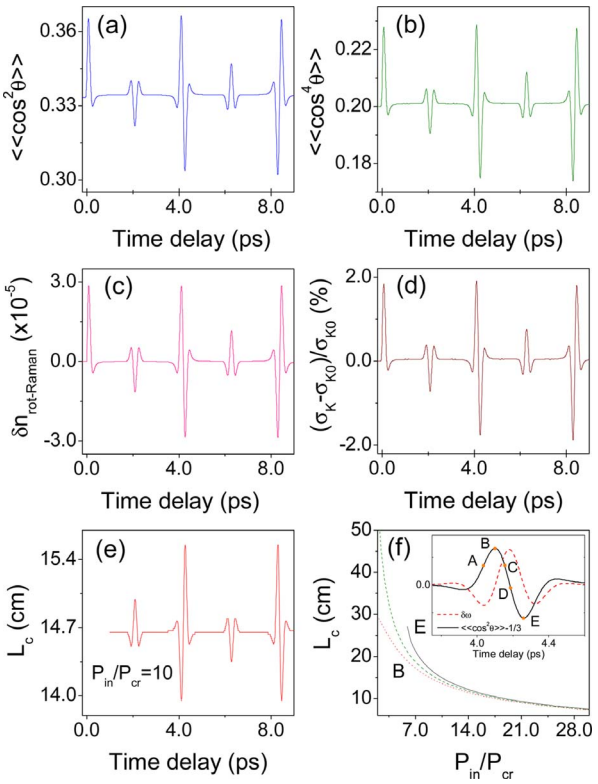

Fig. 1. (Color online) Alignment metrics for pure nitrogen at 1 atm. (a) $\ll\cos^2\theta\gg$ and (b) $\ll\cos^4\theta\gg$, (c) the refractive index $\delta n_{\text{rot-Raman}}$, (d) the normalized ionization cross section, and (e) the collapse length L_c as a function of time delay. (f) The collapse length L_c as a function of $P_{\text{in}}/P_{\text{cr}}$ when the molecules are randomly orientated (dashed curve), or orientated at delays B (dotted curve) and E (solid curve) as labeled in the inset. The corresponding frequency shift induced by the molecular revivals is also plotted in the inset. In the calculations of the collapse length L_c for the collimated probe beam (diameter of 1.0 mm), the pump pulse is focused by a lens (focal length f=40 cm) with an initial beam diameter of 1.6 mm.

tion leads to an additional self-focusing (defocusing) effect for the probe pulse, which linearly depends on the pump intensity for intensities smaller than 10^{14} W/cm^2 [18]. Accordingly, the collapse length L_c, defined as the distance to the nonlinear focus of the probe beam, is modulated [Fig. 1(e)], which is obtained by integrating Eq. (1) without the contributions of dispersion and ionization. Obviously, for parallel orientated molecules the collapse distance is shorter than that for perpendicularly orientated ones. As the molecules are randomly orientated the collapse length is well approximated by the Marburger formula [19]. For prealigned molecules, as shown in Fig. 1(f), this formula still holds for probes with large input powers. However, a noticeable departure from Marburger's collapse distance is observed for probe beams with low input powers and collapse may even be suppressed for a weak probe beam propagating in perpendicularly orientated molecular gas.

The collinearly propagating pump and probe pulses at 800 nm are assumed to have the same polarizations, beam waists, and pulse durations, and are focused using a lens with a focal length of 40 cm. The simulation parameters used here are: $\Delta\alpha$ =1.0 Å^3, $k_0^{(2)}$=0.2 fs^2/cm, $n_2=2.3\times10^{-19}$ cm^2/W, τ_c =350 fs, $\sigma_{K0}=6.31\times10^{-140}$ s^{-1} cm^{22}/W^{11}, and K=11 [1]. The input power and beam diameter of the probe pulse are set as $P_{\text{in}}=2.0\,P_{cr}$ (P_{cr}=4.4 GW for N_2 at 800 nm) and 1.5 mm (FWHM). In the following discussion the probe pulse is tuned to various delays (labeled as A, B, C, D, and E) around the half revival time of the molecular alignment as shown in the inset of Fig. 1(f).

The probe pulse self-focuses at different positions along the propagation direction as its delay relative to the pump pulse is tuned. When its temporal peak matches the revival time for parallel orientation (delay B), the probe pulse self-focuses at a distance shorter by ~2 cm with respect to the case of randomly orientated molecules. In contrast, when the delay is tuned to delay E (perpendicular orientation), the probe pulse focuses at a larger distance and diffracts immediately after the geometric focus of the lens. As shown in Fig. 2(a), for parallel orientation, the filament length (~13 cm) is roughly doubled with respect to the case of randomly orientated molecules (filament length ~7 cm).

In a way similar to the conventional self-phase modulation, here, the phase modulation induced by the temporal evolution of the refractive index (following the molecular alignment revival) plays an impor-

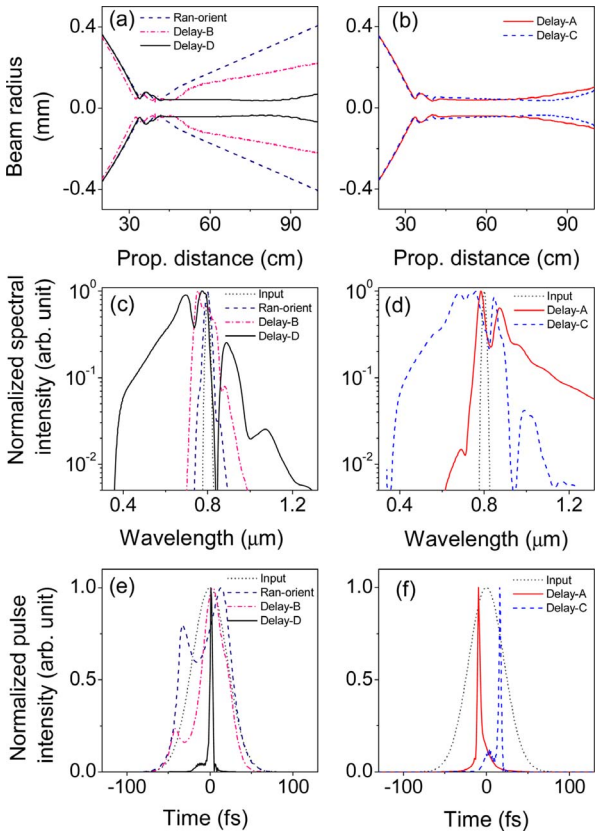

Fig. 2. (Color online) (a),(b) Beam radius evolution of the probe pulse along the propagation distance, (c),(d) the normalized spectra, and (e),(f) the normalized temporal profile of the probe pulse at the end of filamentation in nitrogen when it is delayed to see various molecular orientations.

tant role. The frequency shift induced by the modulated refractive index is plotted in the inset of Fig. 1(f). As a result, for delay A, the probe pulse is redshifted [Fig. 2(d)] and is further compressed down to a few cycles [Fig. 2(f)] via significant spatiotemporal reshaping during its long filamentation stage [Fig. 2(b)] [20]. As shown in Figs. 2(d) and 2(f), for delay C the probe pulse is spectrally blueshifted and a compressed ultrashort pulse is obtained at the end of the filament. The phase modulation is most important at delay D for the maximum slope of the refractive index profile. As shown in Fig. 2(a), a filament of ~55 cm is generated when the probe pulse is tuned to delay D. The probe pulse undergoes significant spectral broadening, which results in an ultrabroad spectrum ranging from 360 to 1300 nm [Fig. 2(c)], and thus in a self-compressed ultrashort pulse of 3.5 fs (FWHM) [Fig. 2(e)]. A small pedestal exists but applications such as the generation of high harmonics and single attosecond pulses were predicted to be rather insensitive to the pedestal [21]. Filamentation in properly aligned molecular gas is therefore an efficient way to force self-compression and generate few-cycle pulses and possibly to overcome the limitations encountered with self-compressed filaments in noble gases such as, e.g., the trade-off between pulse duration and energy of the compressed pulse [22]. Although the maximum refractive index is obtained at delay B the phase modulation effect (proportional to the slope of the refractive index profile) for this delay is quite small, which leads to limited spectrum broadening and thus a short filamentation length as shown in Figs. 2(a) and 2(c).

In summary, we have shown by means of numerical simulations that by using a weak pump pulse as an impulsive rotational Raman excitation and by tuning the delay of an intense probe pulse undergoing filamentation to scan various revival times of molecular alignment induced by the pump, the filamentation dynamics can be readily controlled to obtain desired filament lengths, ultrabroad spectra and pulse self-compression. This provides us an efficient approach to manipulate femtosecond filaments for various promising applications in filamentation nonlinear optics.

During the reviewing process, we became aware of recent experimental works [23] in keeping with the simulations of this paper.

This work was funded in part by the National Natural Science Fund (grants 10774045, 10525416, and 10804032), the National Key Project for Basic Research (grant 2006CB806005), Projects from Shanghai Science and Technology Commission (grants 06JC14025, 06SR07102, and 08ZR1407100), the Program for Changjiang Scholars and Innovative Research Team, and the Shanghai Educational Development Foundation (2008CG29).

References

1. A. Couairon and A. Mysyrowicz, Phys. Rep. **441**, 47 (2007).
2. G. Méjean, J. Kasparian, E. Salmon, J. Yu, J. Wolf, R. Bourayou, R. Sauerbrey, M. Rodriguez, L. Wöste, H. Lehmann, B. Stecklum, U. Laux, J. Eislöffel, A. Scholz, and A. P. Hatzes, Appl. Phys. B **77**, 357 (2003).
3. K. Stelmaszczyk, P. Rohwetter, G. Méjean, J. Yu, E. Salmon, J. Kasparian, R. Ackermann, J.-P. Wolf, and L. Wöste, Appl. Phys. Lett. **85**, 3977 (2004).
4. C. D. Amico, A. Houard, S. Akturk, Y. Liu, J. Le Bloas, M. Franco, B. Prade, A. Couairon, V. T. Tikhonchuk, and A. Mysyrowicz, New J. Phys. **10**, 013015 (2008).
5. S. L. Chin, F. Théberge, and W. Liu, Appl. Phys. B **86**, 477 (2007).
6. A. Couairon, Appl. Phys. B **76**, 789 (2003).
7. I. S. Golubtsov, V. P. Kandidov, and O. G. Kosareva, Quantum Electron. **33**, 525 (2003).
8. H. Stapelfeldt and T. Seideman, Rev. Mod. Phys. **75**, 543 (2003).
9. F. Calegari, C. Vozzi, S. Gasilov, E. Benedetti, G. Sansone, M. Nisoli, S. De Silvestri, and S. Stagira, Phys. Rev. Lett. **100**, 123006 (2008).
10. J. J. Larsen, K. Hald, N. Bjerre, H. Stapelfeldt, and T. Seideman, Phys. Rev. Lett. **85**, 2470 (2000).
11. J. Itatani, J. Levesque, D. Zeidler, H. Niikura, H. Pépin, J. Kieffer, P. B. Corkum, and D. Villeneuve, Nature **432**, 867 (2004).
12. T. Kanai, S. Minemoto, and H. Sakai, Nature **435**, 470 (2005).
13. J. Wu, H. Qi, and H. Zeng, Phys. Rev. A **77**, 053412 (2008).
14. J.-F. Ripoche, G. Grillon, B. S. Prade, M. A. Franco, E. T. J. Nibbering, R. Lange, and A. Mysyrowicz, Opt. Commun. **135**, 310 (1997).
15. E. T. J. Nibbering, G. Grillon, M. A. Franco, B. S. Prade, and A. Mysyrowicz, J. Opt. Soc. Am. B **14**, 650 (1997).
16. I. V. Litvinyuk, K. F. Lee, P. W. Dooley, D. M. Rayner, D. M. Villeneuve, and P. B. Corkum, Phys. Rev. Lett. **90**, 233003 (2003).
17. J. Wu, H. Zeng, and C. Guo, Phys. Rev. A **75**, 043402 (2007).
18. R. Boyd, *Nonlinear Optics*, 2nd ed. (Academic, 2003).
19. J. Marburger, Prog. Quantum Electron. **4**, 35 (1975).
20. A. Mysyrowicz, A. Couairon, and U. Keller, New J. Phys. **10**, 025023 (2008).
21. H. S. Chakraborty, M. B. Gaarde, and A. Couairon, Opt. Lett. **31**, 3662 (2006).
22. A. Zaïr, A. Guandalini, F. Schapper, M. Holler, J. Biegert, L. Gallmann, A. Couairon, M. Franco, A. Mysyrowicz, and U. Keller, Opt. Express **15**, 5394 (2007).
23. S. Varma, Y.-H. Chen, and H.-M. Milchberg, "Trapping and destruction of long-range high-intensity optical filaments by molecular quantum wakes in air," Phys. Rev. Lett. (to be published).